

Supplementary information

Methods

Sample preparation and crystallization

Horse spleen ferritin (Ft) and cisplatin (CDDP) were purchased from Sigma and used without any further purification. CDDP solutions were freshly prepared for each experiment. Stock solution of Ft (code F4503) was stored at 4 °C in 0.15 mM sodium chloride. This solution contained iron in a protein subunit to metal ratio of 1:26.5, according to inductively coupled plasma mass spectrometry (ICP-MS) measurements. The CDDP-encapsulated AFt was prepared following the procedure very similar to that reported by Huang et al.¹: a protein sample (10 mg x mL⁻¹) was first dissociated at pH 13 in the presence of CDDP (protein subunit to metal drug ratio 1:50) and then reassembled at neutral pH. In particular, the protein sample was raised slowly to pH 13 in the presence of CDDP with 0.1 M NaOH, and after 30 min the pH of the resulting solution was adjusted to pH=7 using 1.0 M sodium phosphate buffer. After this process, the sample was extensively dialyzed (5 kDa cutoff) against 10 mM sodium phosphate buffer pH 7.0 and then ultra-filtered (with a 5 kDa cutoff). CDDP-encapsulated sample for experiments was collected after centrifugation at 12000 x g (15 minutes) that remove the abundant precipitates. This procedure was also repeated to obtain a protein sample to be used as “control”. ICP-MS measurements performed on different samples indicate that CDDP-encapsulated Ft contain Pt in a Ft subunit to metal ratio ranging from 1:0.9 to 1:2.3 and an undetectable amount of iron, thus being in the Apo form (AFt), whereas the “control” contain a variable amount of iron (protein subunit to metal ratio in any case < 1:9.9). Experiments carried out in this work were performed using CDDP-encapsulated AFt that contained Pt in 1:2.3 Ft subunit to metal ratio.

The encapsulation of Pt in the AFt core was also confirmed by UV-Vis spectroscopy (see below, Figure S1, as previously done by Guo et al.²). It is possible that more CDDP molecules can be added to the protein using a Ft sample containing a lower amount of iron in the starting stock solution or changing the experimental conditions used to encapsulate the drug, e.g. the protein to metal ratio, the pH and/or the incubation time. Ft concentrations have been determined spectrophotometrically using a molar extinction coefficient reported in a previous work for AFt by Stefanini et al.³ (ϵ 1% 1cm= 9.0), successively validated with the BCA protein assay (BCATM Protein Assay Kit, Pierce).

Crystals of both the control and the CDDP-encapsulated AFt were grown by hanging-drop vapor diffusion technique at 298 K mixing these samples (5-10 mg x mL⁻¹) with equal volumes of a reservoir solution consisting of 0.6-0.8 M (NH₄)₂SO₄, 0.1 M Tris pH 7.4-7.7, 50-60 mM CdSO₄. Best crystals grow within 1-5 days (Figure S3A and 3B). It is interesting to note that crystals of CDDP-encapsulated AFt and of the control are transparent, whereas crystals obtained under the same experimental conditions using the stock solution, which possesses a higher content of iron, are orange (Figure S3C).

X-ray diffraction data collection

X-ray diffraction data for the CDDP-encapsulated AFt and the control were collected from single crystals at XRD1 beamline of Elettra Synchrotron in Trieste, using a detector Pilatus-6M (Dectris) and the wavelength of 1.065 Å. Before being exposed to the X-ray beam, the crystals were soaked for a few seconds in a cryo-solution similar to the mother liquor but containing 25% glycerol and flash cooled at 100 K. Data sets were indexed, integrated, reduced and scaled using XDS⁴ and SCALA.⁵ Data on CDDP-encapsulated AFt were collected and scaled up to 1.45 Å resolution. Data on the control were first scaled at 2.00 Å resolution using XDS⁴ and SCALA⁵ and then to 1.82 Å resolution using iMosflm⁶ and SCALA⁵, following the method suggested by Karplus and Diederichs⁷⁻⁸ and recently successfully applied to the adduct formed in the reaction of cisplatin with hen egg white lysozyme⁹.

X-ray diffraction data were also collected in-house using an additional crystal of CDDP-encapsulated AFt at the CNR Institute of Biostructure and Bioimages, Naples, Italy. This crystal was grown using a sample of CDDP-encapsulated AFt obtained using the same procedure described before. Data were collected using a Saturn944 CCD detector equipped with CuK α X-ray radiation from a Rigaku Micromax 007 HF generator and processed using HKL2000.¹⁰ All the crystals are isomorphous, they are cubic and belong to space group F432 with one Ft monomer in the asymmetric unit. These data were first scaled at 2.45 Å resolution and then rescaled at 2.06 Å resolution. Data collection statistics are reported in Table S1.

Structure resolution and refinement

The structures were solved by molecular replacement method, using the PDB file 2W0O,¹¹ without water molecules and ligands, as starting model and Phaser¹². The refinements were carried out with Refmac5.8,¹³ model building and map inspections were performed using WinCoot.¹⁴ 5% of the data was used for calculation of the R-free value.

The structure of CDDP-encapsulated AFt was refined at 1.45 Å resolution to a Rfactor of 0.145 (Rfree 0.172). The control was first refined at 2.00 Å resolution to Rfactor of 0.143 and Rfree of 0.181 and then using data up to 1.82 Å resolution, but we do not find significant differences in the two models. The refined structures are nearly complete with just one residue absent from the C-terminal region. Refinement statistics are reported in Table S1. Structure validations were carried out using Procheck.¹⁵ Coordinates and

structure factors of the CDDP-encapsulated AFt and of the control were deposited in the Protein Data Bank with PDB codes 5ERJ and 5ERK, respectively. In CDDP-encapsulated AFt a cisplatin fragment was modeled close to His132 side chain (see below).

To further verify the presence of Pt close to His132, a new structure of CDDP-encapsulated AFt was refined against the X-ray diffraction data collected in house. This model was first refined at 2.45 Å resolution and then including data up to 2.06 Å resolution, following the indications by Karplus and Diederichs⁷⁻⁸, recently applied to unambiguously determine the Pt ligands in the X-ray structure of the adduct formed in the reaction between hen egg white lysozyme and cisplatin⁹.

Very interestingly, we found a significant improvement in the description of the CDDP-encapsulated AFt structure refined against the CuK α data, i.e. a better agreement between the model and the structure factors (of course these refinements were carried out excluding the same reflections for R_{free} test set and using exactly the same number of atoms, avoiding any bias, as in reference 7). In particular, the new 2.06 Å resolution model, which has exactly the same number of atoms of previous model, showed a better agreement against the 2.45 Å resolution diffraction data with initial and final factor and R_{free} values respectively of 15.4 % vs 15.8% and 19.9% vs 20.7%.

In order to distinguish between Pt and Cd atoms, we have followed this procedure: a CDDP fragment was located if signals were present in the anomalous difference, 2Fo-Fc and Fo-Fc electron density maps of CDDP-encapsulated AFt, but absent in the same positions in the corresponding maps of the control. A confirmation of the CDDP location assignment was obtained by inspection of the isomorphous difference (Fo-Fo) electron density map, calculated using the phase set of the control. Cd²⁺ ions were located where signals were present in the anomalous difference and Fo-Fc electron density maps of both the CDDP-encapsulated AFt and the control (Table S5). In the assignment of the metal centre, the nature and the arrangement (geometry) of the metal ligands were also considered.

Further insights to discriminate between Pt and Cd atoms were obtained comparing the anomalous electron density maps calculated using the Elettra and the in-house data sets. Between CuK α (1.5418Å) and the wavelength used at Elettra, 1.065Å, the Cd and the Pt signals change in opposite ways. In particular, if one considers the f'' values of these two atoms at these two wavelengths it is possible to note that Cd signal increases from about 2.5 electrons to about 5 electrons and the Pt signal drops from about 10 electrons to about 7 electrons. Thus, the comparison of the anomalous difference Fourier electron density map peaks at the two wavelengths can suggest potential Pt binding sites. This analysis adds further support to our assignment, since it indicates the presence of a potential Pt binding site close to the side chain of His132. Additional potential Pt binding sites identified with this method are close to side chains of Glu11 and Asp80. However, since a peak of anomalous electron density map is observed in these positions in the control, we assign these peaks to Cd²⁺ ions that binds protein with different occupancies. In this respect, we want to follow the indication by Helliwell et al.: "if unsure do not make an assignment".¹⁶

In conclusion, altogether the results of these structural analyses coherently suggest the unambiguous presence of a CDDP binding site close to His132 side chain (Figure S5). We cannot exclude the possibility that other Pt atoms are bound, at low occupancy, replacing Cd²⁺ ions close to Glu11 and Asp80.

To assign the ligands close to Pt, we calculated the omit electron density maps and assigned Pt ligand positions according to map peaks. Since there are no peaks corresponding to Pt ligands in the anomalous maps we exclude the presence of Cl⁻ ions. This is reasonable since it is well known that cisplatin may undergo aquation as, in the absence of high concentrations of chloride ions, Cl⁻ are released from Pt centre. It remains to be determined if Pt coordinates ammonia or aqua ligands. Of course it is very difficult to discriminate N from O atoms using X-ray crystallography, even at high resolution. In our case, the assignment is complicated by the low occupancy (the three peaks have a very low signal :0.25, 0.33, 1.02 e/Å³). However, we tentatively assigned the Pt fragment as –Pt(NH₃)₂OH₂. The refined B-factors for the Pt ligands (43.5 Å² and 45.9 Å² for N; 39.5 for O Å²) suggest that the assignment could be correct.

Comparison with all the other structures of horse spleen ferritin reported in the Protein Data Bank.

In order to compare more strictly the structures of CDDP-encapsulated AFt with those already reported for horse spleen Ft under different experimental conditions, carbon alpha root mean square deviations have been calculated using SwissPDB-Viewer¹⁷ and reported in Table S2. As it can be easily verified by inspection of the values of rmsd in Table S5, the binding of CDDP does not induce large structural variations in AFt molecule. Furthermore, we have also evaluated the binding sites of metals in these structures, by manual inspection of the structures using WinCoot¹⁴. The results of these structural analyses are reported in Table S4.

Evaluation of the structural features of CDDP-encapsulated Ft surface and comparison with the control

To compare the structural features of CDDP-encapsulated Ft with the control and with the starting model, solvent accessible area, volume and distribution of the charge residues on the surface were evaluated using Vadar Server¹⁸, through visual inspection of the structure and calculating the electrostatic potential. Results of these analyses are reported in Table S3 and Figure S6.

Spectrophotometric measurements

UV-vis absorption spectra were recorded using a 0.1 cm optical path-length quartz cell on a JASCO V-560 UV-vis spectrophotometer in the range of 240–700 nm; protein concentration: 0.25 mg x mL⁻¹ in 10 mM sodium phosphate pH 7.0.

Inductively coupled plasma mass spectrometry

Protein samples were suspended in 600 µl HNO₃ and 200 µl HCl overnight at 90 °C. Aliquots of acid solution from each sample were directly analyzed by inductively coupled plasma mass spectrometry (ICP-MS). The solution was then transferred into polystyrene liners, and diluted 1:10 v/v with 5% HNO₃ and finally analyzed with an Agilent 7700 ICP-MS from Agilent Technologies, equipped with a frequency-matching RF generator and 3rd generation Octopole Reaction System (ORS3), operating

with helium gas in ORF. The following parameters were used: radiofrequency power 1550 W, plasma gas flow 14 L x min⁻¹; carrier gas flow 0.99 L x min⁻¹; He gas flow 4.3 mL x min⁻¹. 103Rh was used as an internal standard (50 µg x L⁻¹ final concentration). Multi-element calibration standards were prepared in 5% HNO₃ at 4 different concentrations (1, 10, 50, and 100 µg x L⁻¹). Pt concentration was measured. All the analyses were performed as triplicates.

Zeta potential measurements

Zeta potential of CDDP-encapsulated Ft and of the control was assessed by means of electrophoretic light scattering by using a Zetasizer Nano ZSP (Malvern Instruments, England). Measurements were performed using 0.5 mg x mL⁻¹ protein solutions in 10 mM sodium phosphate buffer, pH 7.0, previously filtered with 220 nm cut-off microfilters, and polystyrene Folded Capillary Zeta cells (Malvern Instruments).

Circular dichroism

Far UV CD spectra were recorded on a Jasco J-715 spectropolarimeter equipped with a Peltier thermostatic cell holder (Model PTC-348WI) in the range of 190–250 nm, using protein concentration of 0.1 mg x mL⁻¹ in 10 mM sodium phosphate pH 7.0.

References

1. X.-T. Ji, L. Huang, H.-Q. Huang. *Journal of Proteomics* 2012, 75, 3145-3157.
2. Z. Yang, X. Wang, H. Diao, J. Zhang, H. Li, H. Sun, Z. Guo. *Chem Commun* 2007, 3453-3455.
3. S. Stefanini, S. Cavallo, C.-Q. Wang, P. Tataseo, P. Vecchini, A. Giartosio, E. Chiancone. *Archives Biochem Biophys* 1996, 325, 54.
4. W. Kabsch. *Acta Crystallogr D Biol Crystallogr*. 2010, 66, 2, 125-32.
5. P.R. Evans. *Acta Crystallogr D Biol Crystallogr*. 2011, 67, 4, 282-92.
6. T.G.G. Battye, L. Kontogiannis, O. Johnson, H. R. Powel, A.G.W. Leslie *Acta Crystallogr D Biol Crystallogr*. 2011, 67, 271-281
7. P.A. Karplus, K. Diederichs. *Science* 2012, 336(6084):1030-3.
8. K. Diederichs. P.A. Karplus. *Acta Crystallogr D Biol Crystallogr*. 2013 Jul;69(Pt 7):1215-22
9. S.W.M. Tanley, A. M. M. Scheurs, L. M. J. Kroon-Batenburg, J. R. Helliwell. *Acta Crystallogr F* 2016, in press. Accepted 14 January 2016
10. Z. Otwinowski and W. Minor, *Methods Enzymol*. 1997, 276, 307-326.
11. N. De Val, J.P. Declercq, C.K. Lim, R.R. Crichton. *J. Inorg. Biochem*. 2012, 112, 77-84.
12. A. J. McCoy, R.W.Grosse-Kunstleve, P. D. Adams, M. D. Winn, L.C. Storoni, R.J. Read. *J Appl Crystallogr*. 2007; 40: 658–674.
13. G. N. Murshudov, P. Skubak, A. A. Lebedev, N. S. Pannu, R. A. Steiner, R. A. Nicholls, M. D. Winn, F. Long, A. A. Vagin, *Acta Crystallogr., Sect. D: Biol. Crystallogr.*, 2011, 67, 355-367.
14. P. Emsley, B. Lohkamp, W. G. Scott, K. Cowtan. *Acta Crystallogr D Biol Crystallogr*. 2010, 66, 486–501.
15. R. A. Laskowski, M. W. Macarthur, D. S. Moss, J. M. Thornton. *J. Appl. Cryst.*, 1993, 26, 283-291.
16. S.W.M. Tanley, A. M. M. Scheurs, L. M. J. Kroon-Batenburg, J. R. Helliwell. *Acta Crystallogr F* 2016, in press. Accepted 15 January 2016
17. L. Willard, A. Ranjan, H. Zhang, H. Monzavi, R. F. Boyko, B. D. Sykes, D. S. Wishart. *Nucleic Acids Res*. 2003, 31(13), 3316–3319.
18. N.Guex, M.C. Peitsch, *Electrophoresis* 1997, 18, 2714-2723

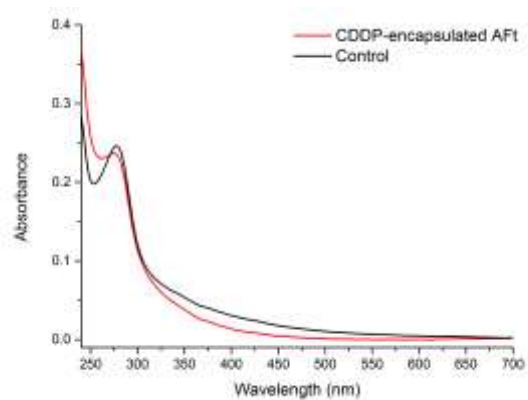


Figure S1. UV-vis absorption spectra of CDDP-encapsulated Aft (red line) and of the control (black line) at $0.25 \text{ mg} \times \text{mL}^{-1}$ in 10 mM sodium phosphate at pH 7.0. The comparison in the region between 250 nm and 280 nm confirms that CDDP is successfully encapsulated in the Aft nanocage, as reported by Guo et al. ².

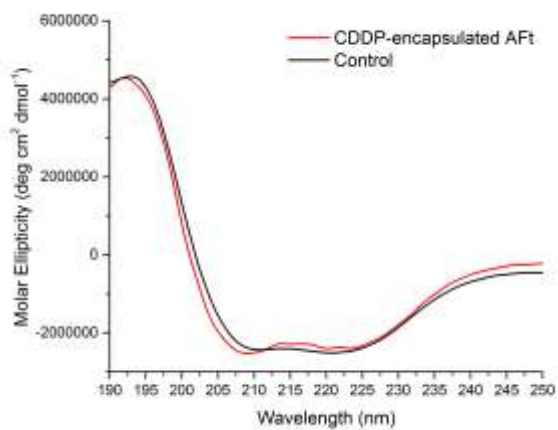


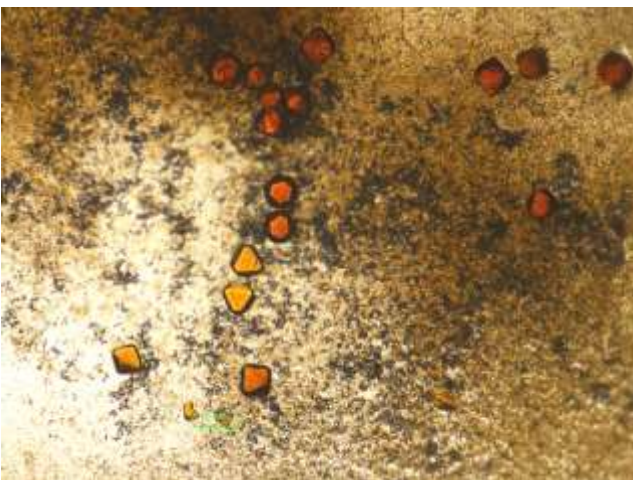
Figure S2. Circular dichroism spectra of control (black line) and CDDP-encapsulated AFt (red line) at $0.1 \text{ mg} \times \text{mL}^{-1}$ in 10 mM sodium phosphate pH 7.0.



A



B



C

Figure S3. Crystals of CDDP-encapsulated AFt (A), of the control (B) and of Ft in the stock solution (C).

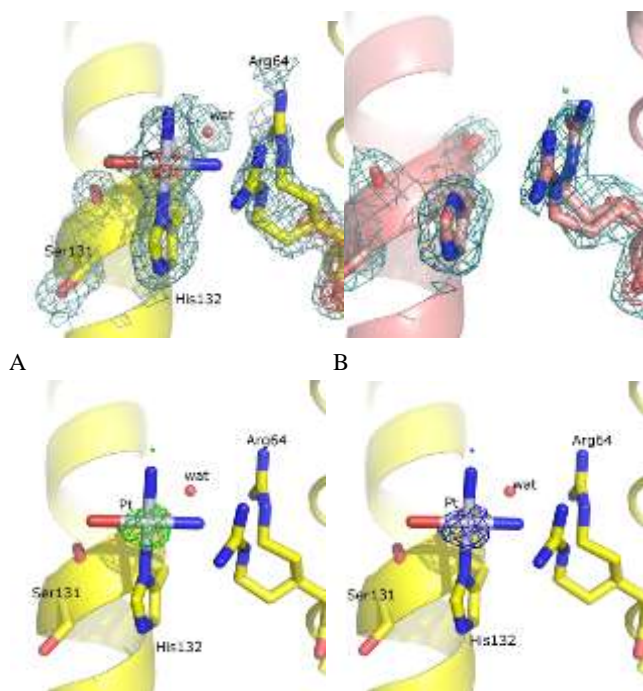


Figure S4. CDDP binding site in the CDDP-encapsulated Aft (yellow). 2Fo-Fc electron density maps of the CDDP-encapsulated Aft (panel A) have been compared to that of Ft in the control (pink, panel B). The maps are contoured at 0.5 σ (cyan) and 2.5 σ (red) level. In panel C and D anomalous difference electron density map and isomorphous difference (Fo-Fo) electron density map are reported, both contoured at 3.5 σ level.

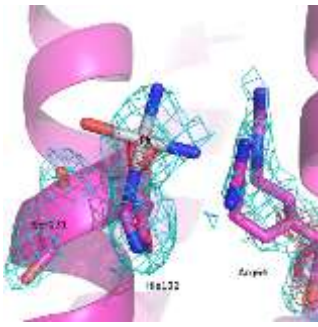
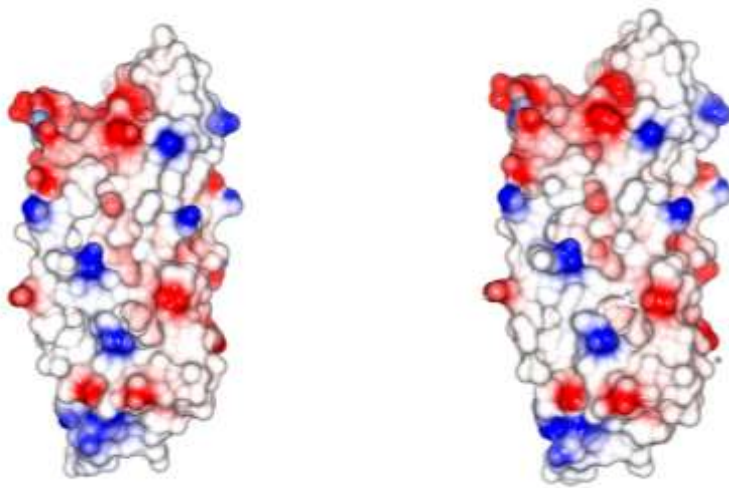


Figure S5. CDDP binding site in the additional CDDP-encapsulated AFt crystal (purple). X-ray diffraction data collection on this crystal were collected at the CNR Institute of Biostructure and Bioimages, Naples, Italy, using a Saturn944 CCD detector equipped with CuK α X-ray radiation from a Rigaku Micromax 007 HF generator. 2Fo-Fc electron density maps are contoured at 0.5 (σ) and 2.0 σ (red) level, respectively.



A

B

Figure S6. Electrostatic potential of the outer surface of monomer of CDDP-encapsulated AFt (A) and of the control (B).

Table S1. Data collection and refinement statistics

	CDDP-encapsulated AFt Elettra data set	Control	CDDP- encapsulated AFt In-house First scaling	Control reprocessed	CDDP-encapsulated AFt In-house reprocessed
PDB code	5ERJ	5ERK	Not deposited		
Data Collection statistics					
Wavelength	1.065	1.065	1.5418	1.065	1.5418
Space group	F432	F432	F432	F432	F432
Unit-cell parameters					
a=b= c (Å)	180.90	180.62	180.29	180.55	182.37
Molecules per a. u.	1	1	1	1	1
Resolution (Å)	104.44-1.45 (1.53-1.45)	104.28-2.00 (2.11-2.00)	104.09-2.45 (2.51-2.45)	63.83-1.82 (1.92-1.82)	32.24-2.06 (2.18-2.06)
Observed reflections	514393	301392	104618	461914	167381
Unique reflections	45325	17642	9736	23188	16494
Completeness (%)	100 (99.8)	100 (100)	99.9 (100)	100 (100)	99.7 (98.2)
half-set correlation $CC_{1/2}$	0.999 (0.867)	0.995 (0.880)	n.a.	0.989 (0.605)	0.950 (0.508)
Anomalous molteplcity	6.0 (4.6)	9.2 (8.5)	5.7 (5.6)	8.0 (7.5)	5.5 (4.4)
Rmerge	0.073 (0.569)	0.080 (0.596)	0.147 (0.502)	0.338 (1.847)	0.525 (1.942)
$I/\sigma(I)$	17.2 (3.5)	10.1 (3.4)	22.6 (7.7)	7.3 (1.6)	3.1 (0.9)
Multiplicity	11.3 (8.9)	17.1 (16.3)	10.7 (10.6)	15.2 (14.8)	10.1 (8.4)
Anomalous completeness	99.9 (99.5)	100 (99.8)	99.9 (99.5)	100 (100)	99.6 (97.3)
Resolution (Å)	104.44-1.45	104.28-2.00	104.09-2.45	63.83-1.82	32.24-2.09
number of reflections in working set	43127	16759	9256	22025	15645
number of reflections in test set	2182	883	468	1153	814
R factor/Rfree /Rall(%)	14.5/17.2/14.7	14.3/18.1/14.5	15.8/20.7/16.1	15.9/19.2/19.2	19.5/24.5/19.7
ΔR factor pair*	-	-	-	0	-0.4
ΔR free pair*	-	-	-	0	-0.8
Number of non-H atoms used in the refinement	1748	1696	1644	1696	1713

Occupancy of Pt centre	0.30	-	0.30	-	0.30
B-factor of Pt centre (Å ²)	53.5	-	76.6	-	75.9
Overall B-factor	18.3	21.1	22.4	17.8	23.2
Deviations from ideality values					
R.m.s.d. bonds (Å)	0.030	0.019	0.016	0.022	0.018
R.m.s.d. angles (Å)	2.55	1.80	1.62	1.93	1.73

* $\Delta R_{\text{factor}} / \Delta R_{\text{free}}$ pairs have been calculated as suggested by Karplus and Diederichs [7-8] and using exactly the same number of atoms.

Table S2. Carbon alpha root mean square deviations for horse spleen Ft structures

PDB code	CDDP-encapsulated AFt	Control												
	5ERJ	5ERK												
1AEW	0.28 Å (170 atoms)	0.30 Å	1DAT	0.64 Å (173 atoms)	0.63 Å	1GWG	0.22 Å (168 atoms)	0.23 Å	1IER	0.60 Å (173 atoms)	0.60 Å	1IES	0.62 Å (173 atoms)	0.62 Å
1XZ1	0.20 Å (168 atoms)	0.20 Å	1XZ3	0.20 Å (168 atoms)	0.21 Å	2GYD	0.20 Å (168 atoms)	0.21 Å	2V2I	0.16 Å (170 atoms)	0.17 Å	2V2J	0.18 Å (170 atoms)	0.19 Å
2V2L	0.16 Å (171 atoms)	0.16 Å	2V2M	0.15 Å (170 atoms)	0.16 Å	2V2N	0.32 Å (171 atoms)	0.26 Å	2V2O	0.32 Å (171 atoms)	0.25 Å	2V2P	0.12 Å (170 atoms)	0.13 Å
2V2R	0.14 Å (170 atoms)	0.16 Å	2V2S	0.33 Å (171 atoms)	0.27 Å	2W00	0.32 Å (170 atoms)	0.31 Å	2Z5P	0.44 Å (171 atoms)	0.39 Å	2Z5Q	0.59 Å (172 atoms)	0.59 Å
2Z5R	0.69 Å (172 atoms)	0.70 Å	3F32	0.19 Å (168 atoms)	0.19 Å	3F33	0.24 Å (168 atoms)	0.25 Å	3F34	0.19 Å (168 atoms)	0.19 Å	3F35	0.22 Å (168 atoms)	0.23 Å
3F36	0.22 Å (168 atoms)	0.21 Å	3F37	0.18 Å (168 atoms)	0.18 Å	3F38	0.19 Å (168 atoms)	0.19 Å	3F39	0.20 Å (168 atoms)	0.20 Å	3RAV	0.21 Å (168 atoms)	0.22 Å
3RD0	0.19 Å (168 atoms)	0.20 Å	3U90	0.22 Å (168 atoms)	0.23 Å	4DE6	0.22 Å (168 atoms)							

Table S3. Structural Features of Ferritin*

	Starting model	Control	CDDP-encapsulated AFt
	2W0O	5ERK	5ERJ
Total Accessible Surface Area (ASA) (\AA^2)	9408.5	9404.1	9321.9
ASA of backbone (\AA^2)	792.8	791.7	787.3
ASA of side chains (\AA^2)	8615.7	8612.4	8534.6
Exposed nonpolar ASA (\AA^2)	5416.0	5429.3	5360.3
Exposed polar ASA (\AA^2)	1738.3	1759.6	1755.3
Exposed charged ASA (\AA^2)	2254.2	2215.3	2206.3
Fraction nonpolar ASA	0.6	0.6	0.6
Fraction polar ASA	0.2	0.2	0.2
Fraction charged ASA	0.2	0.2	0.2
% side ASA hydrophobic	26.0	25.5	25.5
Total volume (packing) (\AA^3)	22810.0	22934.6	22931.1
ACCESSIBLE SURFACE AREA FOR EXTENDED CHAIN*			
Extended nonpolar ASA (\AA^2)	18180.9	18378.9	18340.4
Extended polar ASA (\AA^2)	8474.1	8608.6	8608.6
Extended charged ASA (\AA^2)	4117.4	4199.9	4238.4
Extended side nonpolar ASA (\AA^2)	18049.5	18245.5	18245.5
Extended side polar ASA (\AA^2)	2269.0	2292.9	2292.9
Extended side charged ASA (\AA^2)	4080.3	4163.0	4163.0

*determined using Vadar Server

Table S4. Ligand binding sites on horse spleen ferritin structures deposited in the Protein data bank

PDB CODE	<i>IAEW</i>		<i>IDAT</i>		<i>IGWG</i>		<i>IIER</i>		<i>IIES</i>	
	Ligand	Binding site	Ligand	Binding site	Ligand	Binding site	Ligand	Binding site	Ligand	Binding site
Interactions at distance < 3.50 Å	Cd ²⁺	Asp80	Cd ²⁺	Asp80	Cd ²⁺	Asp80	Cd ²⁺	Glu130	Cd ²⁺	Glu130
	Cd ²⁺	Asp127	Cd ²⁺	Asp127	Cd ²⁺	Glu130	Cd ²⁺	-	Cd ²⁺	
	Cd ²⁺	Glu130	Cd ²⁺	Glu130	I ⁻		Cd ²⁺	Asp80	Cd ²⁺	Glu11 Thr10
	Cd ²⁺	His114			I ⁻					
	Cd ²⁺	His132			I ⁻	Cys48				
	Cd ²⁺	Asp38 Glu45 Cys48			I ⁻	Asp38				
					I ⁻					
					I ⁻					
					I ⁻					
					I ⁻					
PDB CODE	<i>1XZ1</i>		<i>1XZ3</i>		<i>2GYD</i>		<i>2V2I</i>		<i>2V2J</i>	
	Ligand	Binding site	Ligand	Binding site	Ligand	Binding site	Ligand	Binding site	Ligand	Binding site
Interactions at distance < 3.50 Å	Cd ²⁺	Asp80	Cd ²⁺	Asp80	Cd ²⁺	Asp80	Cd ²⁺	Asp127	Cd ²⁺	Asp127
	Cd ²⁺	Glu130	Cd ²⁺	Glu130	Cd ²⁺	Glu130	Cd ²⁺	Asp80	Cd ²⁺	Asp80
	Cd ²⁺	His49	Cd ²⁺	Glu60	Cd ²⁺	Glu53 Glu56	Cd ²⁺	Glu130	Cd ²⁺	Glu130
	Cd ²⁺	Glu88	Cd ²⁺	-	Cd ²⁺	Glu88	Cd ²⁺	Glu130 His114	Cd ²⁺	Glu130 His114
	Cd ²⁺	Glu56 Glu60	Cd ²⁺	Cys48	Cd ²⁺	Glu56 Glu57 Glu60	Cd ²⁺	Asp38 Cys48	Cd ²⁺	Asp38 Cys48
	Cd ²⁺	Glu130	Cd ²⁺	Glu53 Glu56	Cd ²⁺	His114 Cys126	Cd ²⁺	Glu56 Glu57 Glu60	Cd ²⁺	Glu56 Glu57 Glu60
	Halothane	Leu24 Tyr28	Cd ²⁺	Glu130	Cd ²⁺	Glu130	Cd ²⁺	Glu11	Cd ²⁺	Glu11
			isoflurane	Leu24 Leu81	H-diaziflurane	Leu24 Ser27	Cd ²⁺	Glu53 Glu56	Cd ²⁺	Glu53 Glu56
							SO ₄ ²⁻	Asn7	SO ₄ ²⁻	Asn7

							Glycerol	Asp127 Ser131 His132	Glycerol	Arg25 Ser85
									Glycerol	Ala14 Asn17 Arg18 Leu77
									Glycerol	Ser32 Phe35
									Glycerol	Asp38 Ala43
									Glycerol	Ser131 His132
PDB CODE	2V2L		2V2M		2V2N		2V2O		2V2P	
	Ligand	Binding site	Ligand	Binding site	Ligand	Binding site	Ligand	Binding site	Ligand	Binding site
<i>Interactions at distance < 3.50 Å</i>	Cd ²⁺	Asp80	Cd ²⁺	Gln82	Cd ²⁺		Cd ²⁺		Cd ²⁺	-
	Cd ²⁺	Glu130	Cd ²⁺	Glu130	Cd ²⁺	Asp80	Cd ²⁺	Glu130* His114*	Cd ²⁺	Glu130
	Cd ²⁺	Glu130 His114	Cd ²⁺	Glu130 His114	Cd ²⁺	Glu130	Cd ²⁺	Asp80	Cd ²⁺	Glu130 Cys126
	Cd ²⁺	Asp38 Cys48	Cd ²⁺	Asp38 Cys48	Cd ²⁺	Glu130 His114	Cd ²⁺	Glu130	Cd ²⁺	His114 Cys126
	Cd ²⁺	Glu11	Cd ²⁺	Glu11	Cd ²⁺	Asp38 Cys48	Cd ²⁺	Asp38 Cys48	Cd ²⁺	Glu11
	Cd ²⁺	Glu45	Cd ²⁺	Glu45	Cd ²⁺	Glu57 Glu60	Cd ²⁺	Glu57	Glycerol	His132
	Cd ²⁺	Asp127	Cd ²⁺	Asp127	Cd ²⁺	Glu11	Cd ²⁺	Glu11	Glycerol	Asp38 Cys48
	SO ₄ ²⁻	Asn7	SO ₄ ²⁻	Asn7	Cd ²⁺	Glu53 Glu56	Cd ²⁺	Glu53 Glu56	SO ₄ ²⁻	Asn7
	Glycerol	Ser131 His132	Glycerol	Asp135	Glycerol	His132	Cd ²⁺	Glu45		
					Glycerol	Gly90 Tyr36 Gly163	Glycerol	His132 Asp127		
					Glycerol	Ser105	SO ₄ ²⁻	Asn7		
				SO ₄ ²⁻	Asn7					
PDB CODE	2V2R		2V2S		2W0O		2Z5P		2Z5Q	
	Ligand	Binding site	Ligand	Binding site	Ligand	Binding site	Ligand	Binding site	Ligand	Binding site
<i>adist an</i>	Cd ²⁺	Asp127	Cd ²⁺	-	Cd ²⁺	Asp80	Cd ²⁺	Asp80	Cd ²⁺	Asp80

	Cd ²⁺	Asp80	Cd ²⁺	Asp80	Cd ²⁺	Glu130	Cd ²⁺	His132	Pd ²⁺	Glu45 His49 His173
	Cd ²⁺	Glu130	Cd ²⁺	Cys126 Glu130	Cd ²⁺	Glu56 Glu57 Glu60	Pd ²⁺	His114 Cys126 Glu130	Pd ²⁺	Glu45 Cys48 Arg52
	Cd ²⁺	His114 Cys126 Glu130	Cd ²⁺	His114 Cys126 Glu130	Cd ²⁺	Glu11	Pd ²⁺	Cys126Glu130	Pd ²⁺	Glu45 His49 Arg52
	Cd ²⁺	Cys48	Cd ²⁺	Asp38 Cys48	Cd ²⁺	Glu53 Glu56	Pd ²⁺	Asp38 Glu45 Cys48	Pd ²⁺	His114 Cys126
	Cd ²⁺	Glu11	Cd ²⁺	Glu57 Glu60	Cd ²⁺	Glu45*	Pd ²⁺	His114 Cys126 Glu130	Pd ²⁺	Glu53
	Glycerol	Asp127 Ser131 His132	Cd ²⁺	Glu11	Cd ²⁺	Asp38*	Pd ²⁺	His49	Pd ²⁺	Ser2 Asp40* Arg75
	SO ₄ ²⁻	Asn7	Cd ²⁺	Glu53 Glu56	SO ₄ ²⁻	Asn7	Pd ²⁺	Glu45 Cys48	Pd ²⁺	Ser118 Cys126
			Glycerol	Arg39 Asp40			SO ₄ ²⁻	Asn7	Pd ²⁺	Cys126
			Glycerol	His132* Asp127*			SO ₄ ²⁻	Asp146	Pd ²⁺	Glu45 Cys48 Arg52
			SO ₄ ²⁻	Asn7			SO ₄ ²⁻		Glycerol	Thr10 Glu11
							Glycerol			
							Glycerol			
							Glycerol			
PDB CODE	2Z5R		3F32		3F33		3F34		3F35	
	Ligand	Binding site	Ligand	Binding site	Ligand	Binding site	Ligand	Binding site	Ligand	Binding site
Interactions at distance < 3.50 Å	Cd ²⁺	Asp80	Cd ²⁺	Asp80	Cd ²⁺	Asp80	Cd ²⁺	Asp80	Cd ²⁺	Asp80
	Cd ²⁺	Glu60	Cd ²⁺	Glu130	Cd ²⁺	Glu130	Cd ²⁺	Glu130	Cd ²⁺	Glu130
	Pd ²⁺	Ser2 Asp40*	Cd ²⁺	Asp127	Cd ²⁺	Glu53 Glu56	Cd ²⁺	Glu56 Glu57 Glu60	Cd ²⁺	Asp127
	Pd ²⁺	Glu45 His49	Cd ²⁺	Glu56	Cd ²⁺	Glu88	Cd ²⁺	Glu53 Glu56	Cd ²⁺	Glu11
	Pd ²⁺	His124	Cd ²⁺	Glu57	Cd ²⁺	Glu56	Cd ²⁺	Asp127*	Cd ²⁺	Glu53

				Glu60		Glu57 Glu60				Glu56
	Pd ²⁺	Cys48	SO ₄ ²⁻	Asn7	Cd ²⁺	Glu11	2,6-diethylphenol	Leu24 Ser27 Leu81	Cd ²⁺	Glu56 Glu57 Glu60
	Pd ²⁺	His114 Cys126	SO ₄ ²⁻	Asp146	Propofol	Ser27 Arg59	SO ₄ ²⁻	Asn7	Cd ²⁺	Glu88
	Pd ²⁺	Glu45 Cys48			SO ₄ ²⁻	Asn7	SO ₄ ²⁻	Asp146	2,6- diethylphen ol	Ser27 Arg59
	Pd ²⁺	Glu45 Cys48					SO ₄ ²⁻	Arg25*	SO ₄ ²⁻	Asn7
	Pd ²⁺	-					Acetate	Asp127 Ser131 His132 Asp135*	SO ₄ ²⁻	Asp146
	Pd ²⁺	-							SO ₄ ²⁻	Gln86
	Pd ²⁺	Arg64 Glu136								
PDB CODE	3F36		3F37		3F38		3F39		3RAV	
	Ligand	Binding site	Ligand	Binding site	Ligand	Binding site	Ligand	Binding site	Ligand	Binding site
<i>Interactions at distance < 3.50 Å</i>	Cd ²⁺	Asp80	Cd ²⁺	Asp80						
	Cd ²⁺	Glu130	Cd ²⁺	Glu56 Glu57 Glu60						
	Cd ²⁺	Glu130	Cd ²⁺	Glu130	Cd ²⁺	Asp127	Cd ²⁺	Glu130	Cd ²⁺	Glu53 Glu56
	Cd ²⁺	Asp127	Cd ²⁺	Asp127	Cd ²⁺	Glu56 Glu57 Glu60	Cd ²⁺	Asp127	Cd ²⁺	Asp127
	Cd ²⁺	Glu11	Cd ²⁺	Glu11	Cd ²⁺	Glu53 Glu56	Cd ²⁺	Glu56 Glu60	Cd ²⁺	Glu130
	Cd ²⁺	Glu56 Glu57 Glu60	Cd ²⁺	Glu56 Glu57 Glu60	Cd ²⁺	Glu11	Cd ²⁺	Glu11	Cd ²⁺	Glu11
	Cd ²⁺	Glu56	Cd ²⁺	Glu53 Glu56	2,6-dimethylphenol	Ser27 Arg59	Cd ²⁺	Glu53 Glu56	Pentobarbital	Ser27 Arg59
	Cd ²⁺	Glu45	2,6- dimethylphenol	Ser27 Arg59	SO ₄ ²⁻	Asn7	Cd ²⁺	Glu45	SO ₄ ²⁻	Asn7
	2- isopropylphe nol	Tyr28 Arg59	SO ₄ ²⁻	Asn7	SO ₄ ²⁻	Asp146 His147	Phenol	Ser27	SO ₄ ²⁻	Asp146
	SO ₄ ²⁻	Asn7	SO ₄ ²⁻	Asp146			SO ₄ ²⁻	Asn7		

	SO ₄ ²⁻	Asp146	SO ₄ ²⁻	Arg25*			SO ₄ ²⁻	Asp146 His147		
			Acetate	Arg168 Leu171						

§ Sodium Dodecyl-sulphate

* Symmetry related residue

Table S5. Interactions of Cd²⁺ ions in CDDP-encapsulated AFt and in the control

	CDDP-encapsulated AFt 5ERJ	Control 5ERK	CDDP-encapsulated AFt (crystal 2)
Atom	Interactions at distance < 3.00 Å	Interactions at distance < 3.00 Å	Interactions at distance < 3.00 Å
CD 1	Occupancy 0.40 B-factor 22.9 Å ² OE1 Glu11 (2.28 Å) OE2 Glu11 (2.55 Å) WAT 129 (2.17 Å) WAT 183 (2.31 Å) Cl 3 (2.60 Å)	Occupancy 0.40 B-factor 42.4 Å ² OE1 Glu11 (2.67 Å) OE2 Glu11 (2.26 Å) WAT 129 (2.84 Å) WAT 319 (2.58 Å) Cl 3 (2.49 Å)	Occupancy 0.40 B-factor 41.4 Å ² OE1 Glu11 (2.71 Å) OE2 Glu11 (2.50 Å) WAT 129 (2.01 Å) WAT 183 (2.55 Å) Cl 4 (2.64 Å)
CD 2	Occupancy 0.40 B-factor 43.7 Å ² OE1 Glu53 (2.91 Å) OE2 Glu53 (2.38 Å) OE1 Glu56 (2.50 Å) WAT 237 (2.49 Å)	Occupancy 0.30 B-factor 51.9 Å ² OE1 Glu53 (2.50 Å) OE2 Glu53 (2.58 Å) OE1 Glu56 (2.54 Å) WAT 315 (2.34 Å)	Occupancy 0.40 B-factor 51.8 Å ² OE1 Glu53 (2.93 Å) OE2 Glu53 (2.85 Å) OE1 Glu56 (2.38 Å) WAT 302 (2.89 Å)
CD 3	Occupancy 0.30 B-factor 44.0 Å ² OE2 Glu56 (2.37 Å) OE1 Glu60 (2.75 Å) OE2 Glu60 (2.22 Å) Occupancy 0.20 B-factor 35.80 Å ² OE1 Glu60 (2.38 Å) WAT 191 (2.17 Å)	Occupancy 0.30 B-factor 69.1 Å ² OE1 Glu60 (2.46 Å) WAT 292 (2.77 Å)	Occupancy 0.30 B-factor 56.4 Å ² OE2 Glu56 (2.88 Å) OE1 Glu60 (2.79 Å) OE2 Glu60 (2.74 Å) Occupancy 0.20 B-factor 60.5 Å ² OE1 Glu60 (2.39 Å) WAT 191 (2.37 Å) Cl 6 (2.65 Å)
CD 4 at the binary axis	Occupancy 0.40 B-factor 10.5 Å ² OD1 Asp80 (2.30 Å)	Occupancy 0.50 B-factor 15.7 Å ² OD1 Asp80 (2.42 Å)	Occupancy 0.50 B-factor 16.4 Å ² OD1 Asp80 (2.47 Å)

	OD2 Asp80 (2.45 Å) OD1 Asp80* (2.32 Å) OD2 Asp80* (2.50 Å) CI 1 (2.44 Å) CI 1* (2.49 Å) Occupancy 0.10 B-factor 19.5 Å ² OD1 Asp80 (2.09 Å) OD2 Asp80 (1.85 Å) OD1 Asp80* (2.20 Å) OD2 Asp80* (2.07 Å) CI 1 (2.85 Å) CI 1* (3.03 Å)	OD2 Asp80 (2.08 Å) OD1 Asp80* (2.48 Å) OD2 Asp80* (2.27 Å) CI 2 (2.61 Å) CI 2* (2.34 Å)	OD2 Asp80 (2.22 Å) OD1 Asp80* (2.46 Å) OD2 Asp80* (2.35 Å) CI 1 (2.46 Å) CI 1* (2.65 Å)
CD 5	Occupancy 0.30 B-factor 44.4 Å ² OE2 Glu88 (2.29 Å) WAT 81 (1.93 Å) WAT 181 (2.24 Å) WAT 187* (2.63 Å)	Occupancy 0.20 B-factor 61.0 Å ² OE2 Glu 88 (2.28 Å) WAT 313 (2.46 Å) WAT187* (2.72 Å)	-
CD 6	Occupancy 0.40 B-factor 45.3 Å ² OG Ser131 (2.69 Å) OD1 Asp127 (2.97 Å) WAT 196 (2.45 Å) WAT 197 (2.46 Å) WAT 230 (1.96 Å)	Occupancy 0.40 B-factor 69.3 Å ² OD1 Asp127 (2.87 Å) WAT 245 (2.46 Å) WAT 311 (2.18 Å)	Occupancy 0.40 B-factor 62.5 Å ² OD1 Asp127 (2.42 Å) WAT 196 (2.79 Å)
CD 7	Occupancy 0.50 B-factor 42.1 Å ² NE2 His132 (2.50 Å) OD2 Asp135* (2.88 Å) WAT 196 (2.37 Å) WAT 197 (2.51 Å) WAT 275 (1.71 Å)	Occupancy 0.40 B-factor 39.9 Å ² NE2 His132 (2.66 Å) WAT 245 (2.19 Å) WAT 246 (2.24 Å) WAT 294 (2.12 Å) WAT 295 (2.42 Å)	Occupancy 0.50 B-factor 60.2 Å ² NE2 His132 (2.70 Å) WAT196 (2.29 Å) WAT197 (2.46 Å) WAT275 (2.41 Å)
CD 8	Occupancy 0.20	Occupancy 0.20	Occupancy 0.30

at the ternary axis	<p style="text-align: center;">B-factor 42.7 Å²</p> OE1 Glu130 (2.41 Å) OE1 Glu130* (2.41 Å) OE1 Glu130* (2.41 Å) Cl 2 (1.89 Å) Cl 2* (1.89 Å) Cl 2* (1.89 Å)	<p style="text-align: center;">B-factor 46.5 Å²</p> OE1 Glu130 (2.47 Å) OE1 Glu130* (2.47 Å) OE1 Glu130* (2.43 Å) Cl 2 (2.34 Å) Cl 2* (2.32 Å) Cl 2* (2.28 Å)	<p style="text-align: center;">B-factor 61.3 Å²</p> OE1 Glu130 (2.29 Å) OE1 Glu130* (2.25 Å) OE1 Glu130* (2.26 Å) Cl 5 (2.87 Å) Cl 5* (2.89 Å) Cl 5* (2.89 Å)
CD 9	<p style="text-align: center;">Occupancy 0.40 B-factor 56.5 Å²</p> NE2 His114 (2.71 Å) WAT 265* (2.89 Å)	<p style="text-align: center;">Occupancy 0.20 B-factor 59.1 Å²</p> WAT 252* (2.54 Å) Cl 1* (2.92 Å)	<p style="text-align: center;">Occupancy 0.40 B-factor 72.6 Å²</p> NE2 His114 (2.75 Å) WAT 265* (2.76 Å) Cl 5* (2.70 Å)
CD 10	<p style="text-align: center;">Occupancy 0.30 B-factor 42.1 Å²</p> OE1 Glu63/A (2.71 Å) OE2 Glu63/A (2.28 Å) OE2 Glu63/B (2.27 Å) WAT 85 (1.67 Å) WAT 247 (2.45 Å)	<p style="text-align: center;">Occupancy 0.20 B-factor 51.5 Å²</p> OE1 Glu63 (2.58 Å)	<p style="text-align: center;">Occupancy 0.30 B-factor 62.5 Å²</p> OE1 Glu63 (2.89 Å) WAT 85 (2.37 Å) WAT 219 (2.81 Å)
CD 11	<p style="text-align: center;">Occupancy 0.30 B-factor 30.9 Å²</p> SG Cys48 (1.98 Å) WAT 231 (1.95 Å)	<p style="text-align: center;">Occupancy 0.30 B-factor 33.6 Å²</p> SG Cys48 (2.08 Å) WAT 310 (2.03 Å)	<p style="text-align: center;">Occupancy 0.30 B-factor 25.2 Å²</p> SG Cys48 (2.00 Å) WAT 231 (1.79 Å)
CD 12	<p style="text-align: center;">Occupancy 0.40 B-factor 56.8 Å²</p> OE2 Glu45/B (2.39 Å) WAT 255 (2.19 Å) Cl 5 (2.72 Å)	<p style="text-align: center;">Occupancy 0.30 B-factor 73.9 Å²</p> OE1 Glu45 (2.51 Å) WAT 235 (2.15 Å)	<p style="text-align: center;">Occupancy 0.40 B-factor 66.7 Å²</p> OE2 Glu45 (2.61 Å) WAT 282 (2.91 Å)
CD 13	<p style="text-align: center;">Occupancy 0.20 B-factor 44.1 Å²</p> OE1 Glu45/A (2.19 Å) NE2 His49 (2.25 Å)	<p style="text-align: center;">Occupancy 0.20 B-factor 44.1 Å²</p> OE2 Glu45/A (2.46 Å) NE2 His49 (2.66 Å) WAT 236 (2.94 Å)	<p style="text-align: center;">Occupancy 0.20 B-factor 57.4 Å²</p> OE1 Glu45/A (2.20 Å) NE2 His49 (2.53 Å)

* Symmetry related residue